Petrophysical approach for estimating porosity, clay volume, and water saturation in gas-bearing shale: A case study from the Horn River Basin, Canada

Taeyoun KIM[1)2)], Seho HWANG[2)] & Seonghyung JANG[2)*)]

[1)] Department of Petroleum Resources Technology, University of Science and Technology, 217 Gajeong-ro, Yuseong-gu, Daejeon 34113, Republic of Korea;

[2)] Korea Institute of Geoscience and Mineral Resources, 124 Gwahang-no, Yuseong-gu, Daejeon 34132, Republic of Korea;

[*)] Corresponding author: shjang@kigam.re.kr

Abstract

Shale gas exists partly as a gas adsorbed to clay mineral and partly as a free gas within the pores. To evaluate a shale gas reservoir and calculate total gas content, it is essential to accurately analyze porosity, clay volume, and water saturation. In this study, we estimate these factors for the Horn River Basin using various types of well log data such as density log, sonic log, resistivity log, and neutron porosity log. Because a simple density porosity equation results in unreasonable fluid densities, we estimate porosity using total organic carbon. Based on brittleness, an empirical equation for clay volume is defined. Because the correlation coefficient between core-tested clay volume and water saturation is greater than 0.9, the empirical equation for water saturation is also defined in terms of brittleness. For the shale gas reservoir in the Horn River Basin, porosity can be calculated by using a linear equation with the density log, and clay volume and water saturation can be calculated by using a linear relationship with Young's modulus and Poisson's ratio. This study suggests that porosity, clay volume, and water saturation models can be established using the elastic model built on seismic inversion.
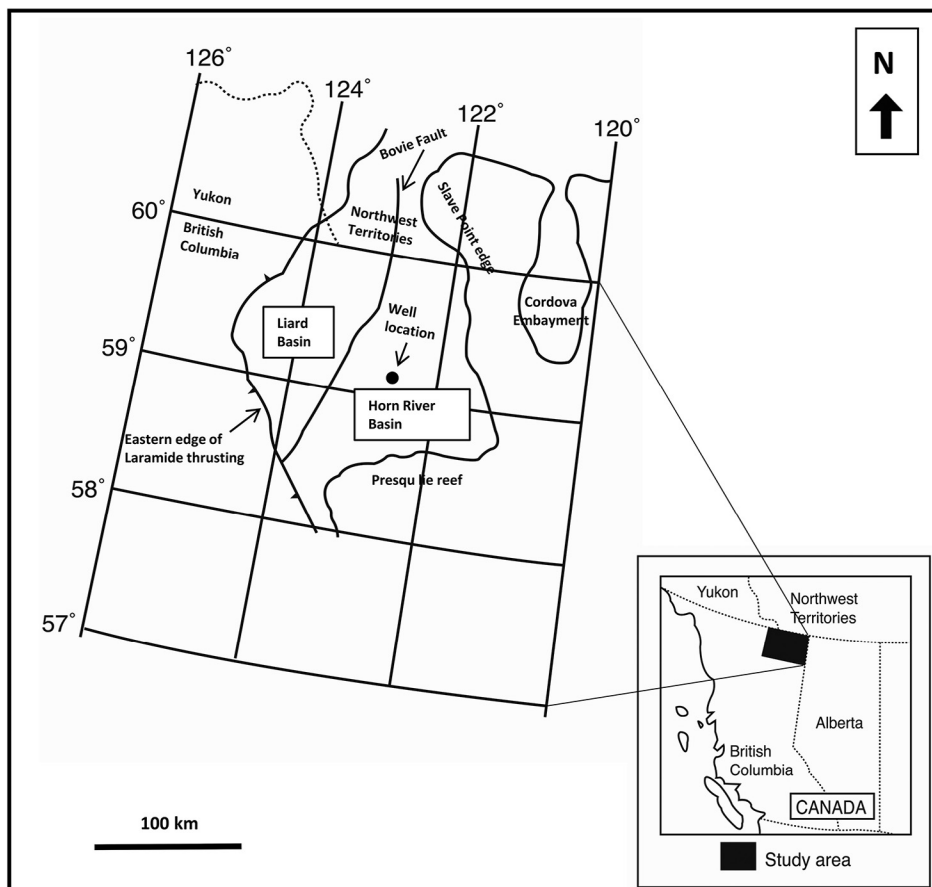
1. Introduction

Shale, which is fine-grained and organic-rich, serves as source rock and at the same time as reservoir rock in which shale gas can be found (Ross and Bustin, 2007). Because shale has very small pores with weak connections between them, and also has low permeability, conventional reservoir evaluation is not appropriate (Kennedy et al., 2012). It is necessary to analyze the thermal maturity of organic matter so that the type and quantity of generated hydrocarbon can be examined. Shale gas is present in the reservoir as both free and adsorbed gas (Tian et al., 2013). Free gas fills the pores or spaces between mineral particles constituting the shale, while adsorbed gas is held on the surface of clay minerals and organic matter. Thus, free gas can flow freely through the pores or cracks, while adsorbed gas can flow only after being desorbed as a result of lower pressure in the reservoir rock. To evaluate a shale gas reservoir, the total amount of free gas can be calculated by multiplying the volume of a reservoir by its porosity and gas saturation. The amount of adsorbed gas under various pressures can be estimated using the organic content in the reservoir. To evaluate the hydrocarbon potential, it is also necessary to determine the rock type, mineral content, brittleness index, gas saturation, and pressure variation. Depth, volume, and geological structure of the reservoir can be determined by processing and interpreting seismic data. In characterizing a shale gas reservoir, well log data is used to analyze porosity, permeability, gas saturation, etc., as they relate to core analysis results (Heidari et al., 2011; Quirein et al., 2012;

Saneifar et al., 2013). Based on these results, it becomes possible to detect intervals with a high chance of having shale gas and to determine which interval should be suitable for horizontal drilling for optimal shale gas production. However, because hydrocarbon content in a shale gas reservoir is different from that in a conventional gas reservoir, it requires the use of a more detailed petrophysical model involving organic matter for interpreting well log data (Glorioso and Rattia, 2012; Alfred and Vernik, 2013; Holmes et al., 2014). Khalid et al. (2010) showed variation in properties along horizontal well of shale gas reservoir in Canada. Kam et al. (2015) applied history matching simulations based on 3D geocellular model in the Horn River Basin. Ahmad and Haghighi (2013) proposed a water saturation model appropriate for the range of total porosity in shale gas reservoirs. Ghawar and Elburas (2015) suggested that Poisson's ratio is relevant to the clay content in shaly sand reservoirs. By using the Waxman-Smits equation (Waxman and Smits, 1968), Sarihi and Vargas-Murillo (2015) estimated water saturation in tight rock reservoirs, including those containing clay minerals.

In this study, we estimate the porosity, clay volume, and water saturation of a shale gas reservoir in the Horn River Basin using various types of logs and core plugs analysis data from single well. In addition, we suggest that the porosity, clay volume, and water saturation models can be established using the elastic model which is built on seismic inversion.

2. Geologic and field data background

The Horn River Basin is located in northeast British Columbia, Canada, and is known to have shale gas reservoirs containing free gas and adsorbed gas (Chen and Hannigan, 2016) (Figure 1). It may contain one of the largest unconventional gas accumulations in North America, with an ultimate potential for unconventional gas resources of 450 trillion cu ft (BC Ministry of Energy and Mines, 2011). The basin fill contains three main shale formations of great interest as gas reservoirs, each of which was deposited when sea levels were rising during the Devonian Period of the Paleozoic Era. From the youngest to the oldest, these three formations are known as Muskawa, Otterpark and Evie; they are the siliciclastic deeper-water age-equivalents to the shallow water Leduc, Swanshill and Slavepoint carbonate formations, respectively. The shaly Fort Simpson formation overlays the Muskawa formation; the Keg River carbonate formation, which serves as a fracture barrier, underlays the Evie formation (Johnson et al. 2011) (Figure 2). Characteristics of each shale layer are relatively similar, although thickness varies depending on the location. In the upper part of the Otterpark layer, a carbonate fan is present : there is a fracture barrier layer with abundant at the bottom (Kam et al., 2015). Thus, the Muskwa and Evie layers, which have relatively more organic matter and silicate mineral, are the main targets for recovering shale gas (Ratcliffe et al., 2012). The well log data used in this study are composed of a P-wave velocity log, a S-wave velocity log, a density log, a neutron porosity log, a resistivity log, a uranium content log, an Elemental Capture Spectroscopy (ECS) grain density log, and an ECS clay volume log (Figure 3). In addition, X-ray diffraction (XRD) analysis, core porosity analysis, core total organic carbon (TOC) analysis, and core water saturation analysis have been performed for 41 core plug samples together with well log data that were obtained from the same location.

Figure 1: Map of Horn River Basin and adjacent areas, including well location (modified after Dong et al., 2015).
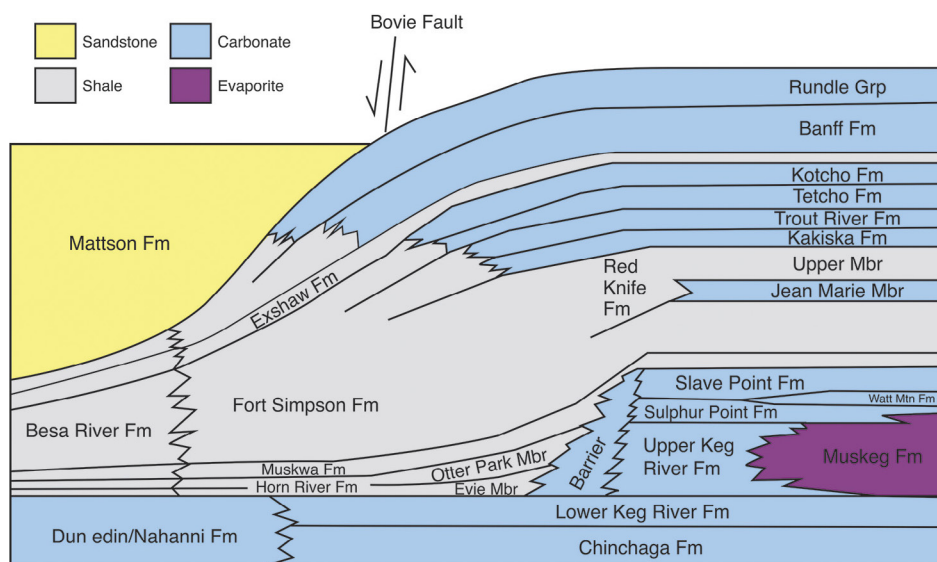

Figure 2: Mississippian/Devonian stratigraphy of Liard and Horn River Basin in northeastern British Columbia (modified after Chalmers et al., 2012). Study formations are Muskwa, Otterpark, and Evie.
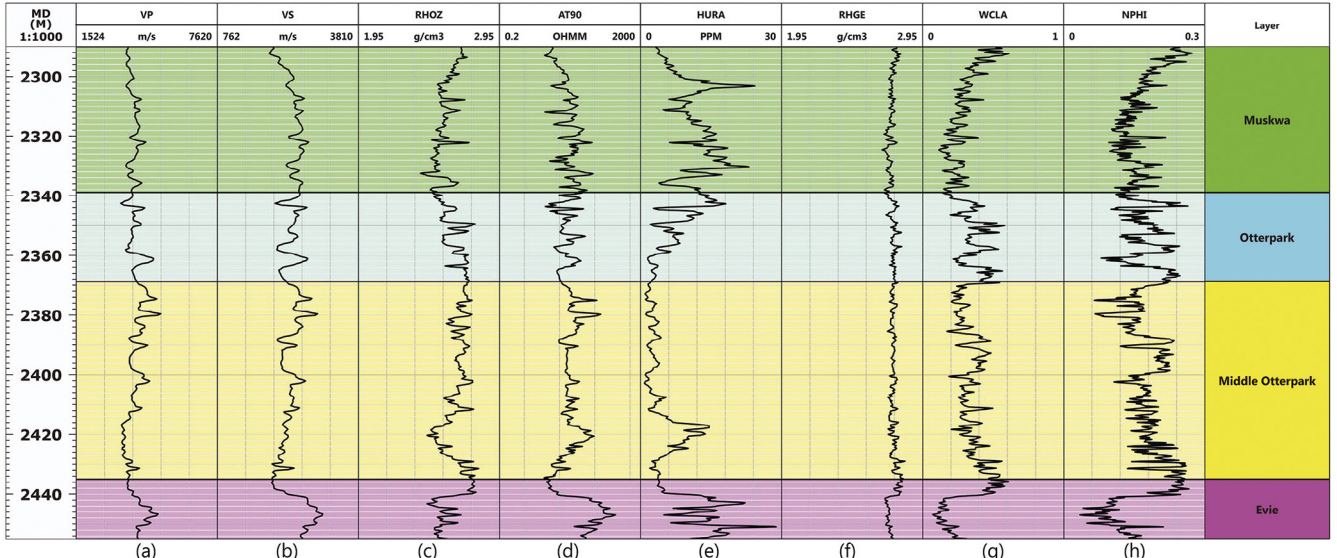
Figure 3: Well logs for the layers of the study area showing (a) P-wave velocity, (b) S-wave velocity, (c) density, (d) resistivity, (e) uranium content, (f) ECS grain density, (g) ECS clay volume, and (h) neutron porosity.
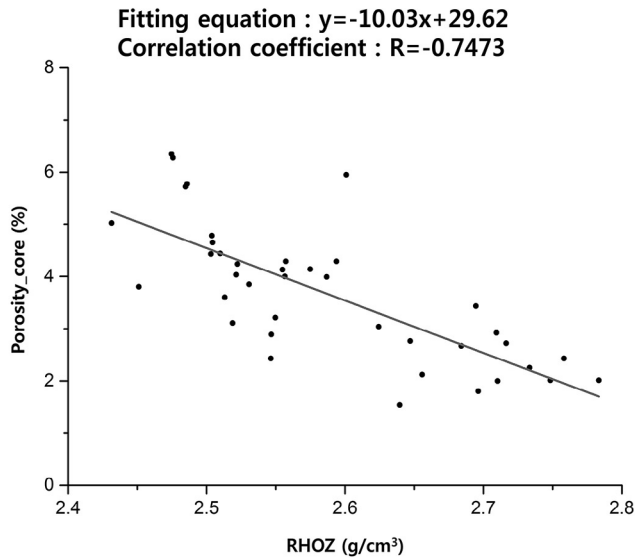
Figure 4: Crossplot of core-tested porosity versus the density log.

3. Porosity analysis

Since porosity is one of the input variables for calculating water saturation, it must be correctly calculated. When shale has high clay content, the neutron porosity log is overestimated due to the hydrogen effect of clay. Therefore, the density log is used to calculate the porosity of a shale gas reservoir; the equation is as follows:

$$\Phi = \frac{\rho_m - \rho_b}{\rho_m - \rho_f} \tag{1}$$

where Φ is porosity (dimensionless), ρ_b is bulk density (g/cm³), ρ_m is matrix density (g/cm³), and ρ_f is fluid density (g/cm³).

In gas reservoirs, the bulk density calculation results in a value lower than the actual value because of gas effects, and

the porosity calculated by using the density log is greater than the actual value. Thus, the fluid density applied in Equation (1) should be lower than 1.05 g/cm³. Figure 4 shows a crossplot between core-tested porosity and the density log. A relation between them is derived as follows:

$$\Phi(\%) = -10.03 \times RHOZ + 29.62 \tag{2}$$

where *RHOZ* is the density log value (g/cm³).

Figure 5b shows a comparison between the porosity calculated by using Equation (2) and the core-tested porosity. The range of calculated porosity is found to be approximately 3% to 5% and is highly correlated to the core-tested porosity. Comparing Equations (1) and (2), it appears that the matrix density is 2.953 g/cm³ and the fluid density is –7.017 g/cm³, but this is unreasonable. If the fluid density is greater than zero, the porosity is overestimated. Figure 5c shows a comparison between porosity obtained by applying the density and ECS grain density logs to Equation (1) and core-tested porosity. In this case, the applied fluid density is –1.042 g/cm³, which is the average across the 41 core plugs.

Even when using the ECS grain density log, porosity can be overestimated, if fluid density is greater than zero. Sondergeld et al. (2010) suggested allowing for TOC in the porosity calculation as follows:

$$\Phi = \frac{\rho_m - \rho_b \left(\rho_m \dfrac{w_{TOC}}{\rho_{TOC}} - w_{TOC} + 1 \right)}{\rho_m - \rho_f + w_{TOC} \times \rho_f \times \left(1 - \dfrac{\rho_m}{\rho_{TOC}} \right)} \tag{3}$$

where ρ_{TOC} is the organic carbon density (g/cm³) and W_{TOC} is the weight fraction of TOC from log measurements (dimensionless).
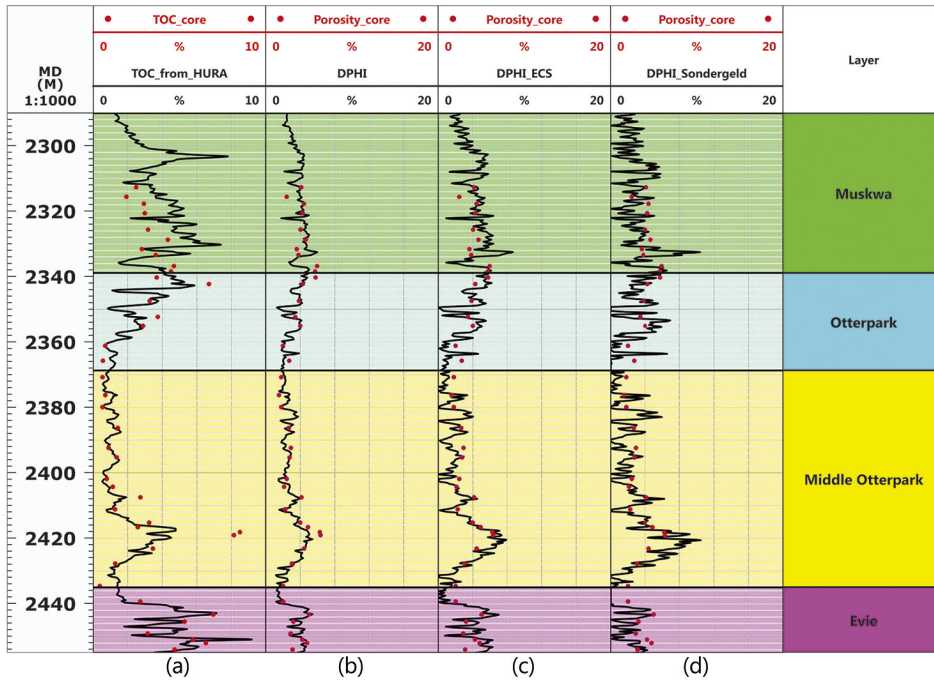
Figure 5: Well logs showing (a) core-tested TOC comparing with the TOC log calculated by using uranium porosity log. Core-tested porosity compared with (b) density porosity, (c) density porosity calculated by using the ECS grain density log, and (d) density porosity calculated by Sondergeld et al.'s (2012) equation.
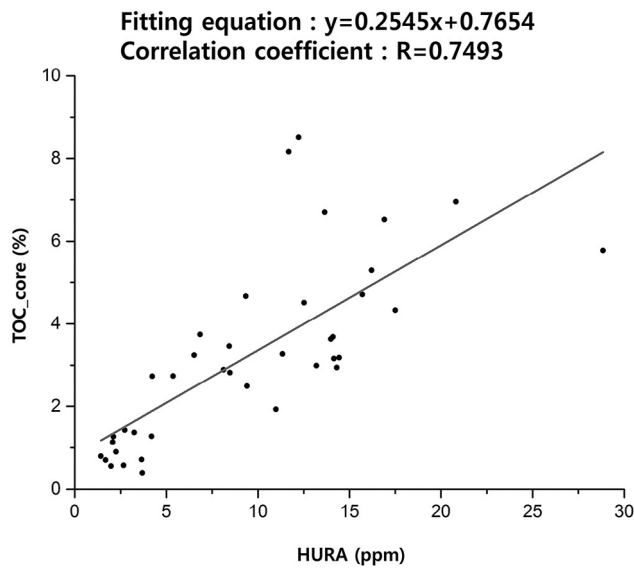
Figure 6: Crossplot of core-tested TOC versus the uranium content log.

In the case of a shale gas reservoir, an interval with high uranium content log values can be estimated to have a high organic material content (Glorioso and Rattia, 2012). Figure 6 is a crossplot between the uranium content log and core-tested TOC. A linear relationship between them is defined as follows:

$$TOC\,(\%) = -0.245 \times HURA + 0.7654 \qquad (4)$$

where *HURA* is the uranium content log value (ppm).

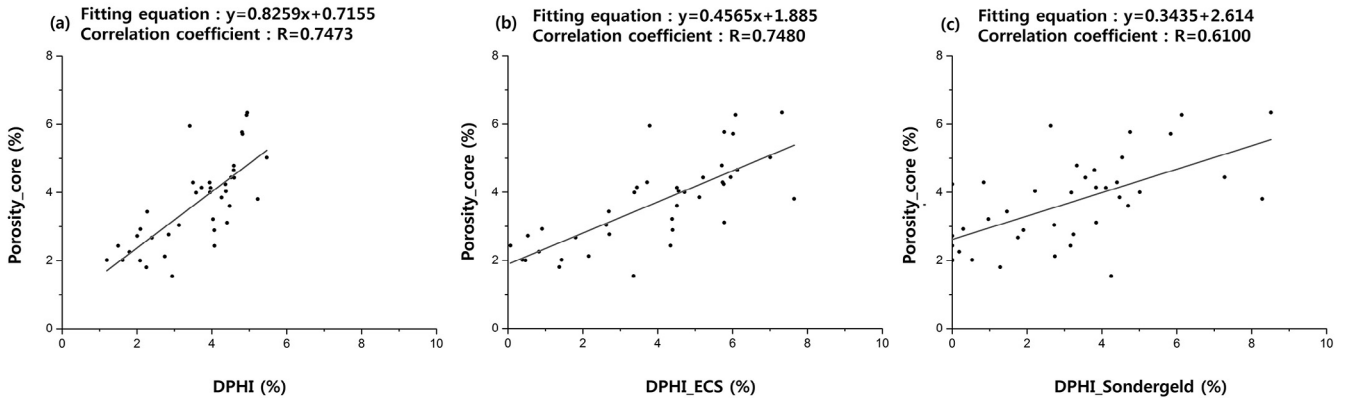TOC is calculated by using Equation (4), and the result is used

as input for Equation (3). Figure 5a shows a comparison between the core-tested TOC and the TOC calculated by using Equation (4). Figure 5d shows a comparison between the core-test porosity and the porosity determined by applying the density, ECS grain density, and TOC logs to Equation (3). It is assumed that TOC density is 1.3 g/cm³ and fluid density is 0.7 g/cm³. It is not necessary to use a fluid density value that is less than 0 in a porosity equation that allows for TOC, such as Equation (3). Figure 7 shows a crossplot between the three calculated density porosities and the core-tested porosity. Even if the Equation (1) results in an unreasonable fluid density that is less than zero, the correlation coefficient with core-tested porosity is greater than when calculated by using Sondergeld's equation (Sondergeld et al., 2010). Furthermore, the range found for density porosity calculated without the ECS grain density log is more similar to the core-tested porosity than to that calculated with the ECS grain density log.
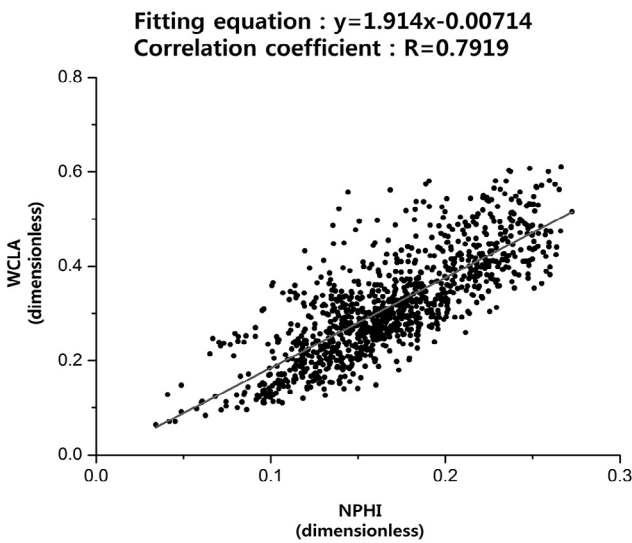
4. Clay volume analysis

Because clay in shale gas reservoirs reduces porosity, the clay volume should be considered to calculate water saturation correctly. The two most common methods used to calculate clay volume are based on gamma ray response and the difference between neutron and density porosities. However, the presence of minerals high in uranium content results in erroneously high clay volume calculations. The difference between neutron and density porosities is another accepted indicator of clay volume that works well in elastic depositional sequences. In clean sandstones, the neutron and density porosity values are similar and often overlap, assuming that each porosity curve is computed on a sandstone matrix. In shale, the porosity curves diverge because of a lower shale matrix density, which causes a reduction in density porosity and higher neutron porosity as a result of the hydrogen index effect in clay. The neutron-density porosity equation (Bhuyan and Passey, 1994) is as follows:

$$V_{CLAY} = \frac{\dfrac{NPHI_{matrix} - NPHI}{NPHI_{matrix} - NPHI_{fluid}} - \dfrac{RHOB_{matrix} - RHOB}{RHOB_{matrix} - RHOB_{fluid}}}{\dfrac{NPHI_{matrix} - NPHI_{shale}}{NPHI_{matrix} - NPHI_{fluid}} - \dfrac{RHOB_{matrix} - RHOB_{shale}}{RHOB_{matrix} - RHOB_{fluid}}} \qquad (5)$$

(a) Fitting equation : y=0.8259x+0.7155
Correlation coefficient : R=0.7473

(b) Fitting equation : y=0.4565x+1.885
Correlation coefficient : R=0.7480

(c) Fitting equation : y=0.3435+2.614
Correlation coefficient : R=0.6100

Figure 7: Crossplots of core-tested porosity versus (a) density porosity, (b) density porosity calculated by using the ECS grain density log, and (c) porosity calculated by using the density porosity equation from Sondergeld et al.'s (2012).

Fitting equation : y=1.914x-0.00714
Correlation coefficient : R=0.7919

Figure 8: Crossplot of the ECS clay volume log versus the neutron porosity log.

Figure 9: Well logs showing core-tested clay volume compared with the clay volume log calculated by using (a) the neutron-density porosity method, (b) the neutron porosity log, and (c) the multivariable fitting method.
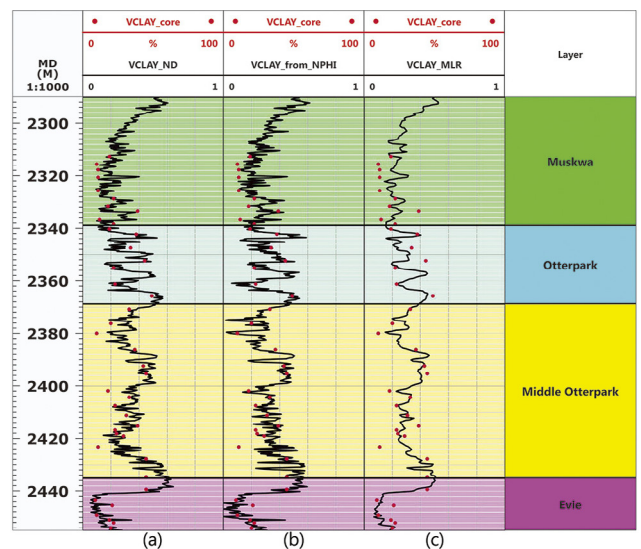
where V_{CLAY} is the clay volume (dimensionless), $NPHI$ is the neutron porosity log (dimensionless), $NPHI_{fluid}$ is the neutron porosity log of the fluid, $NPHI_{shale}$ is the neutron porosity log of shale, $NPHI_{matrix}$ is the neutron porosity log of the matrix, $RHOB_{matrix}$ is the bulk density of the matrix, $RHOB_{fluid}$ is the bulk density of the fluid, and $RHOB_{shale}$ is the bulk density of shale.

It is assumed that the neutron porosity log value of the matrix is 0, the neutron porosity log of shale is 0.4, the bulk density of shale is 2.8 g/cm³, and the bulk density of the fluid is 0.7 g/cm³. Because the neutron porosity log is heavily affected by the clay volume, a crossplot between the neutron porosity log and the ECS clay volume log is composed (Figure 8). Since the correlation coefficient is greater than 0.8, the clay volume equation using the neutron porosity log is derived as follows:

$$V_{CLAY} = 1.914 \times NPHI - 0.00714 \qquad (6)$$

where $NPHI$ is the neutron porosity log value.

In general, shale can be either ductile or brittle, depending on the type of contained clay. Illite tends to be brittle, whe-

reas smectite is more likely to be ductile. Rickman et al. (2008) defined the brittleness index equation using Young's modulus and Poisson's ratio as follows:

$$BI_{Rickman\ (2008)} = \frac{1}{2}\left(\frac{YM-1}{8-1} + \frac{PR-0.4}{0.15-0.4}\right) \qquad (7)$$

where YM is Young's modulus (Mpsi), and PR is Poisson's ratio (dimensionless).

Allowing for these characteristics, we attempt to establish a clay volume logging model using Young's modulus and Poisson's ratio, as follows:

$$V_{CLAY} = a \times YM + b \times PR + c \qquad (8)$$

Using the ECS clay volume log, the well logging Young's modulus, and Poisson's ratio in the least squares fitting equation, the empirical factors to calculate the V_{CLAY} for the shale gas re-
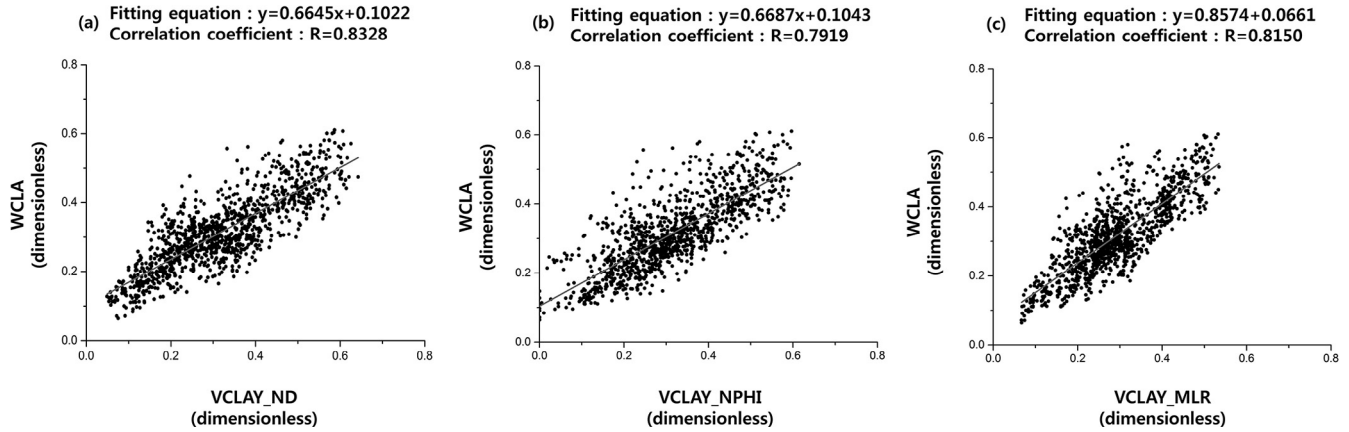
Figure 10: Crossplots of the ECS clay volume log versus clay volume log calculated by using (a) the neutron-density porosity method, (b) the neutron porosity log, and (c) the multivariable fitting method.

servoir in the Horn River Basin are: $a = -0.05257$, $b = 1.322$, $c = 0.2886$, and $R = 0.8150$.

Figures 9a, b, and c denote the clay volumes that are calculated by using Equations (5), (6), and (8), respectively, and these are plotted against the ECS clay volume log (Figure 10). It is more accurate to use the linear equation between the neutron porosity log and the ECS clay volume log than to use the neutron-density porosity approach. Because the correlation coefficient is larger than 0.8, the clay volume calculation method using Young's modulus and Poisson's ratio is reasonable.

5. Water saturation analysis

In reservoir evaluation, water saturation is crucial, because it is directly related to hydrocarbon saturation. A clear relationship between the resistivity log and water saturation is required for an accurate determination of water saturation. Because resistivity is high in the matrix, it depends entirely on the fluid present within the pores of the reservoir. Archie (1942) proposed the following equation based on experimental data using clean sand:

$$S_w = \left[\frac{a \times R_w}{R_t \times \Phi^m} \right]^{\frac{1}{n}} \qquad (9)$$

where S_w is water saturation (dimensionless), R_w is the resistivity of formation water at the formation temperature (ohm·m), R_t is the true formation resistivity (ohm·m), a is the tortuosity factor (dimensionless), m is the cementation exponent (dimensionless), and n is the saturation exponent (dimensionless).

Many studies have used Archie's equation to determine water saturation not only for clean sand but also for shaly

sand or carbonate rock. Arguing that this equation is applicable only to clean sand, Ara et al. (2001) suggested a modified version for other cases. In addition, Archie's equation was found to be unsuitable for shale, because clay ions affect stratum resistivity (Waxman and Smits, 1968). Moreover, water saturation is high with increased clay bound water, thus it is necessary to use the water saturation equation considering clay volume for shale gas reservoir. Waxman and Smits (1968) suggested a water saturation equation that allows for both clay-bound water and free water:

$$\frac{a}{R_t \times \Phi^m} = \frac{1}{R_w} \times S_w^{n} + \frac{\Phi_{sh} \times V_{sh}}{\Phi} \times \left(\frac{1}{\Phi_{sh}^{m} \times R_{sh}} - \frac{1}{R_w} \right) S_w^{(n-1)} \qquad (10)$$

where Φ_{sh} is the porosity of shale (dimensionless), R_{sh} is the resistivity of shale (ohm·m), and V_{sh} is the volume of shale (dimensionless). Instead of the V_{sh}, the V_{CLAY} can be used.

In Equations (9) and (10), a and m can be determined in an
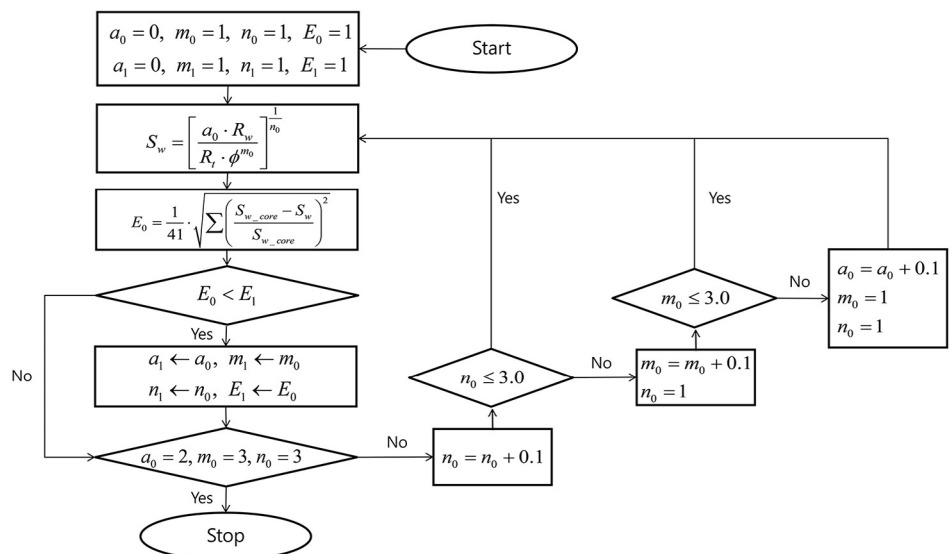
Figure 11: Block diagram of the numerical method for determining the tortuosity factor, cementation exponent, and saturation exponent.
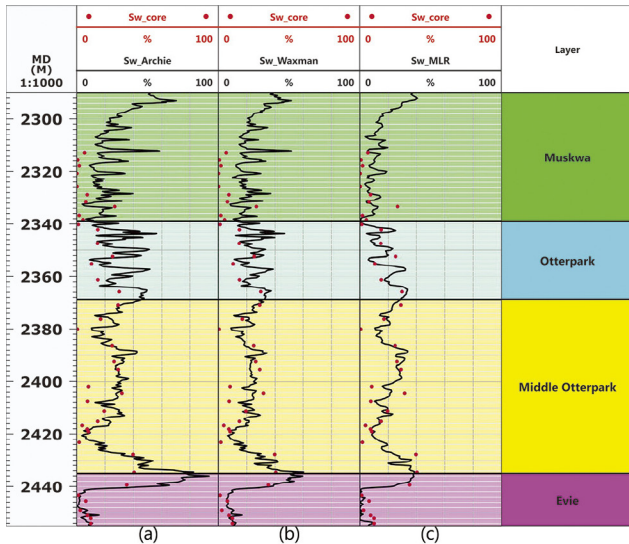
Figure 12: Well logs showing core-tested water saturation compared with the water saturation log calculated by using (a) the Archie's equation (Archie, 1942), (b) the Waxman-Smits equation (Waxman and Smits, 1968), and (c) the multivariable fitting method.
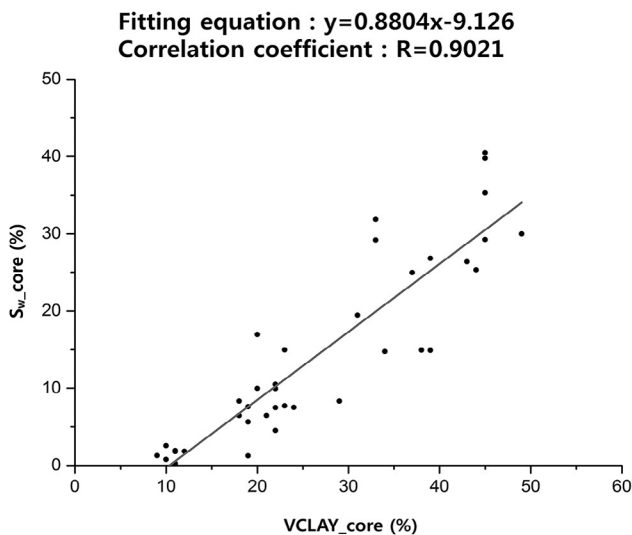
Figure 13: Crossplot of the core-tested water saturation versus the core-tested clay volume.

interval without sudden increase in the resistivity well logging value, with stable borehole diameter and complete water saturation. The value of n varies with the salinity of the pore water and the water saturation of the clay. In general, n is set to 2 in conventional reservoirs, corresponding to solidified rock (Donaldson and Siddiqui, 1989). In this study, a numerical method is used to determine a, m, and n (Figure 11). The search range for a is 0 to 2; for both m and n, it is 1 to 3. In the numerical method, when the variables are 0.5, 1.1, and 2.2, respectively, the error versus core-tested water saturation is minimized. Allowing for the temperature and salinity of the formation water, its resistivity is found to be 0.05 ohm·m. The water saturation is calculated by using Equations (9) and (10), and the results are compared with the core-tested water saturation. We found that in the Muskwa formation, both equa-

tions result in greater values for water saturation than those found in the core analysis (Figures 12a and b). Figure 13 shows a crossplot between the clay volume from XRD tests and the core-tested water saturation. The correlation coefficient is greater than 0.9, and water saturation increases as clay volume increases. Because the clay volume log using Young's modulus and Poisson's ratio seems reasonable, a water saturation equation is similarly defined:

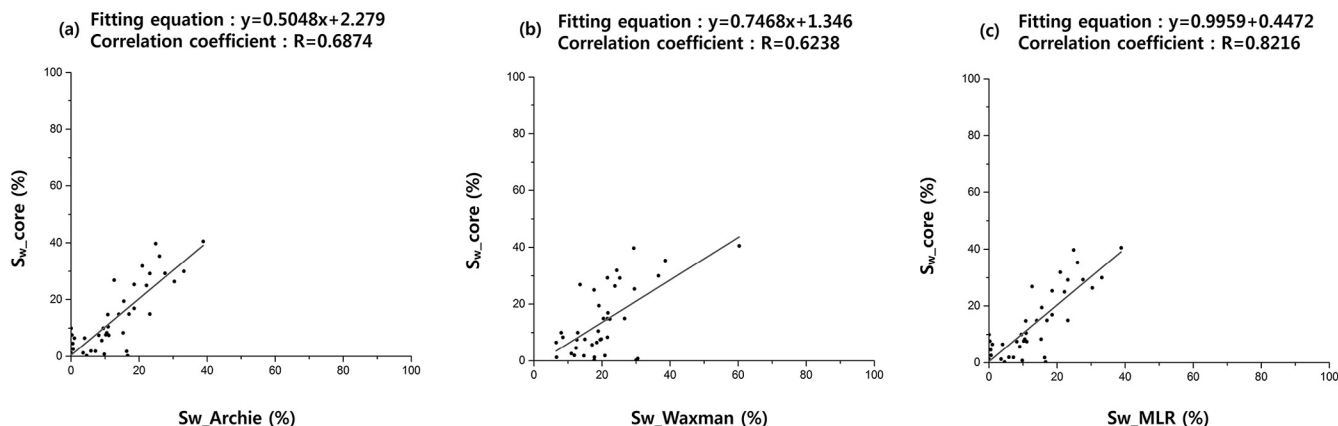$$S_w \,(\%) = a \times YM + b \times PR + c \qquad (11)$$

Using core-tested water saturation, well logging Young's modulus, and Poisson's ratio in the least squares fitting equation, the empirical factors to calculate water saturation for the shale gas reservoir in the Horn River basin are: a = -3.801, b = 190.1, c = -6.837, and R = 0.8216.

Figure 12c shows a comparison between water saturation calculated by Equation (11) and core-tested water saturation. With a few exceptions for some intervals, we can presume a good fit between the core-tested water saturation and water saturation calculated by using Equation (11). Figure 14 shows a crossplot between water saturation determined by Equations (9), (10), and (11) and core-tested values. Although the Waxman-Smits equation takes clay volume into account, the correlation coefficient of the water saturation calculated by using Archie's equation which does not consider clay volume is larger. In addition, the correlation coefficient is much larger when allowing for only the elastic characteristics of clay volume, as shown in Equation (11), and not resistivity and porosity.

6. Discussion

We estimated the porosity, clay volume, and water saturation of a shale gas reservoir in the Horn River Basin in various ways, utilizing well log data and core analysis results. The density porosity equation has a disadvantage in that it must assume negative fluid density. This assumption is also necessary to calculate porosity using the density and ECS grain density logs. Therefore, an additional variable, other than bulk density, grain density, or fluid density is necessary to calculate porosity in shale gas reservoirs.

Reasonable fluid density can be assumed when porosity is calculated by using Sondergeld's equation (Sondergeld et al., 2010, 2012) which considers TOC contents. Although ECS clay volume log was established, we also conducted a clay volume analysis using the neutron porosity and density logs. Clay volume estimated from the linear equation between the neutron porosity and ECS clay volume logs is more closely correlated than that derived from the neutron porosity and density logs. To establish the water saturation model for the study area, we applied Archie's equation (Archie, 1942) as well as Waxman-Smits equation (Waxman and Smits, 1968). The latter yields a lower correlation coefficient, though the difference is not significant. Even though the target of this study area is shale gas reservoir, the water saturation can be calculated by using Archie's equation instead of the Waxman-Smits equation.

(a) Fitting equation : y=0.5048x+2.279
Correlation coefficient : R=0.6874

(b) Fitting equation : y=0.7468x+1.346
Correlation coefficient : R=0.6238

(c) Fitting equation : y=0.9959+0.4472
Correlation coefficient : R=0.8216

Figure 14: Crossplots of the core-tested water saturation versus the water saturation log calculated by using (a) the Archie's equation (Archie, 1942), (b) the Waxman-Smits equation (Waxman and Smits, 1968), and (c) the multivariable fitting method.

7. Conclusions

The purpose of this study is defining empirical equations using elastic properties to calculate porosity, clay volume, and water saturation. We verified that the correlation coefficient between the density log and the core-tested porosity is larger than 0.7. Therefore, an empirical equation can be defined by using only the density log to establish the well logging porosity model for the study area. Since clay volume is related to brittleness index, an empirical equation can be defined by using the well logging Young's modulus and Poisson's ratio from the aspect of brittleness to establish the well logging clay volume model for this area. The correlation coefficient between core-tested clay volume and core-tested water saturation is greater than 0.9. Based on this, an empirical equation can be defined in terms of Young's modulus and Poisson's ratio, as we did in the clay volume analysis.

In summary, since each shale layer is extensively distributed in the Horn River Basin, porosity is calculated by using a linear equation with the density log, and clay volume and water saturation are calculated by using a linear relationship with Young's modulus and Poisson's ratio in the study area. Consequently, we can build a porosity, clay volume, and water saturation model using empirical equations which we have defined, and an elastic model based on seismic inversion. For a future study, we will build a porosity and water saturation model based on seismic inversion and evaluate shale gas resources and reserves in the study area.

Acknowledgements

References

Ahmad, M. and Haghighi, M., 2013. Water Saturation Evaluation of Murteree and Roseneath Shale Gas Reservoirs, Cooper Basin, Australia Using Wire-line Logs, Focused Ion Beam Milling and Scanning Electron Microscopy. In: Society of Petroleum Engineers (ed.), Proceedings of the SPE Unconventional Resources Conference and Exhibition-Asia Pacific, 11–13th November 2013, Brisbane, Australia, pp. 1–20.

Alfred, D. and Vernik, L., 2013. A new petrophysical model for organic shales. Petrophysics, 54/3, 240–247.

Ara, T.S., Talabani, S., Vaziri, H. and Islam, M., 2001. In-depth investigation of the validity of the Archie Equation in carbonate rocks. In: Society of Petroleum Engineers (ed.), Proceedings of the SPE Production and Operations Symposium, 24–27th March 2001, Oklahoma City, Oklahoma, USA, pp. 1–10.

Archie, G.E., 1942. The electrical resistivity log as an aid in determining some reservoir characteristics. Transactions of the AIME, 146/1, 54–62.

Bhuyan, K. and Passey, Q., 1994. Clay estimation from GR and neutron-density porosity logs. In: Society of Petrophysicists and Well-Log Analysts (ed.), Proceedings of the SPWLA 35th Annual Logging Symposium, 19–22th Jun 1994, Tulsa, Oklahoma, USA, pp. 1–15.

B.C. Ministry of Energy and Mines, 2011. Ultimate Potential for Unconventional natural Gas in Northeastern British Columbia's Horn River Basin, Oil and gas Reports 2011-1, Victoria, B.C., pp. 1–39.

Chalmers, G.R.L., Ross, D.J.K. and Bustin, R.M., 2012. Geological controls on matrix permeability of Devonian Gas Shales in the Horn River and Liard basins, northeastern British Columbia, Canada. Internation Journal of Coal Geology, 103, 120–131. http://dx.doi.org/10.1016/j.coal.2012.05.006

Chen, Z. and Hannigan, P., 2016. A Shale Gas Resource Potential Assessment of Devonian Horn River Strata Using a Well-Performance Method. Canadian Journal of Earth Sciences, 53/2, 156–167. http://dx.doi.org/ 10.1139/cjes-2015-0094

Donaldson, E. and Siddiqui, T., 1989. Relationship between the Archie saturation exponent and wettability. SPE formation evaluation, 4/3, 359–362.

Dong, T., Harris, N.B., Ayranci, K., Twermlow, C.E. and Nassichuk, B.R., 2015. Porosity characteristics of the Devonian Horn River shale, Canada: Insights from lithofacies classification and shale composition. Internation Journal of Coal Geology, 141, 74–90. http://dx.doi.org/10.1016/j.coal.2015.03.001

Ghawar, B.M.B. and Elburas, F.S., 2015. Poisson's Ration, Deep Resistivity and Water Saturation Relationships for Shaly Sand Reservoir, SE Sirt, Murzuq and Gadames Basins, Libya (Case study). Journal of Geography and Geology, 7/1, 20. http://dx.doi.org/10.5539/jgg.v7n1p20

Glorioso, J. and Rattia, A., 2012. Unconventional Reservoirs: Basic Petrophysical Concepts for Shale Gas. SPE Paper 153004. In: Society of Petroleum Engineers (ed.), Proceedings of the Society of Petroleum Engineers, 20–22th March 2012, Richardson, Texas, Vienna, Austria, pp. 1–38.

Heidari, Z., Torres-Verdin, C. and Preeg, W.E., 2011. Quantitative method for estimating total organic carbon and porosity, and for diagnosing mineral constituents from well logs in shale-gas formations. In: Society of Petrophysicists and Well-Log Analysts (ed.), Proceedings of the SPWLA 52nd Annual Logging Symposium, 14–18th May 2011, Colorado Springs, Co, USA, pp. 1–15.

Holmes, M., Holmes, D. and Holmes, A., 2014. A New Petrophysical Model To Define Porosity Components Of Unconventional Reservoirs, Using Standard Open-hole Triple Combo Logs. In: Society of Petroleum Engineers (ed.), Proceedings of the SPE Western North American and Rocky Mountain Joint Meeting, 16–18th April 2014, Denver, Colorado, USA, pp. 1–13.

Johnson, M.F., Walsh, W., Budgell, P.A. and Davidson, J.A., 2011. The Ultimate Potential for Unconventional Gas in the Horn River Basin: Integrating Geological Mapping with Monte Carlo Simulations. In: Society of Petroleum Engineers (ed.), Proceedings of the Canadian Unconventional Resources Conference, 15–17th November 2011, Calgary, Alberta, Canada, pp. 1–17.

Kam, P., Nadeem, M., Novlesky, A., Kumar, A. and Omatsone, E.N., 2015. Reservoir Characterization and History Matching of the Horn River Shale: An Integrated Geoscience and Reservoir-Simulation Approach. Journal of Canadian Petroleum Technology, 54/6, 475–488. http://dx.doi.org/10.2118/171611-PA

Kennedy, R.L., Knecht, W.N. and Georgi, D.T., 2012. Comparisons and contrasts of shale gas and tight gas developments, North American experience and trends. In: Society of Petroleum Engineers (ed.), Proceedings of the SPE Saudi Arabia Section Technical Symposium and Exhibition, 8–11th April 2012, Al-Khobar, Saudi Arabia, pp. 1–27.

Khalid, S., Faurschou, K., Zhao, X., Gorchynski, T. and Marechal, F., 2010. Mapping Key Revervoir Properties Along Horizontal Shale Gas Wells. In: Society of Petroleum Engineers (ed.), Proceedings of the Canadian Unconventional Resources and International Petroleum Conference, 19–21th October 2010, Calgary, Alberta, Canada, pp. 1–17.

Quirein, J.A., Murphy, E.E., Praznik, G., Witkowsky, J.M., Shan-non, S. and Buller, D., 2012. A Comparison of Core and Well Log Data to Evaluate Porosity, TOC, and Hydrocarbon Volume in the Eagle Ford Shale. In: Society of Petroleum Engineers (ed.), Proceedings of the SPE Annual Technical Conference and Exhibition, 8–10th October 2012, San Antonio, Texas, USA, pp. 1–13.

Ratcliffe, K., Woods, J. and Rice, C., 2012. Determining well-bore pathways during multilateral drilling campaigns in shale resource plays: an example using chemostratigraphy from the Horn River Formation, British Columbia, Canada. In: T. Mares (ed.), Proceedings of the Eastern Australasian Basins Symposium IV, 10–14th September 2012, Brisbane, QLD, Australia, pp. 143–148.

Rickman, R., Mullen, M.J., Petre, J.E., Grieser, W.V. and Kundert, D., 2008. A practical use of shale petrophysics for stimulation design optimization: All shale plays are not clones of the Barnett Shale. In: Society of Petroleum Engineers (ed.), Proceedings of the SPE Annual Technical Conference and Exhibition, 21–24th September 2008, Denver, Colorado, USA, pp. 1–11.

Ross, D.J. and Bustin, R.M., 2007. Shale gas potential of the lower jurassic gordondale member, northeastern British Columbia, Canada. Bulletin of Canadian Petroleum Geology, 55/1, 51–75. http://dx.doi.org/ 10.2113/gscpgbull.55.1.51

Saneifar, M., Aranibar, A. and Heidari, Z., 2013. Rock Classification in the Haynesville Shale-Gas Formation Based on Petrophysical and Elastic Rock Properties Estimated from Well Logs. In: Society of Petroleum Engineers (ed.), Proceedings of the SPE Annual Technical Conference and Exhibition, 30th September–2nd October 2013, New Orleans, Louisiana, USA, pp. 1–12.

Sarihi, A. and Vargas-Murillo, B., 2015. A Method to Compute Water Saturation in Tight Rocks Accounting for Conductivity of Clay Minerals. In: Society of Petroleum Engineers (ed.), Proceedings of the Abu Dhabi International Petroleum Exhibition and Conference, 9–12th November 2015, Abu Dhabi, UAE, pp. 1–14.

Sondergeld, C.H., Newsham, K.E., Comisky, J.T., Rice, M.C. and Rai, C.S., 2010. Petrophysical considerations in evaluating and producing shale gas resources. In: Society of Petroleum Engineers (ed.), Proceedings of the SPE Unconventional Gas Conference, 23–25th February 2010, Pittsburgh, Pennsylvania, USA, pp. 1–34.

Tian, H., Zhang, S., Liu, S. and Chen, J., 2013. Overmature Shale Gas Storage Capacity Evaluation. In: International Petroleum Technology Conference (ed.), Proceedings of the IPTC 2013: International Petroleum Technology Conference, 26–28th March 2013, Beijing, China, pp. 1–4.

Waxman, M. and Smits, L., 1968. Electrical conductivities in oil-bearing shaly sands. Society of Petroleum Engineers Journal, 8/2, 107–122.

Taeyoun KIM[1) 2)], Seho HWANG[2)] & Seonghyung JANG[2)*)]

[1)] Department of Petroleum Resources Technology, University of Science and Technology, 217 Gajeong-ro, Yuseong-gu, Daejeon 34113, Republic of Korea;

[2)] Korea Institute of Geoscience and Mineral Resources, 124 Gwahangno, Yuseong-gu, Daejeon 34132, Republic of Korea;

[*)] Corresponding author: shjang@kigam.re.kr